Functional & Integrative Genomics (2025) 25:107
https://doi.org/10.1007/s10142-025-01617-x

RESEARCH

N4-acetylcytidine modification of LncRNA GFOD1-AS1 promotes high glucose-induced dysfunction in human dermal microvascular endothelial cells through stabilization of DNMT1 protein

Jingjing Yuan[1] · Lusha Li[1] · Yang Lv[2] · Wenjun Yang[1]

Received: 24 January 2025 / Revised: 13 May 2025 / Accepted: 14 May 2025

Abstract

Emerging evidence supports that angiogenesis is essential for the wound healing of diabetic foot ulcer (DFU), and high glucose (HG)-induced dysfunction of human dermal microvascular endothelial cells is a key factor that hinders angiogenesis. However, the underlying mechanisms by which HG leads to the dysfunction of human dermal microvascular endothelial cells has not been fully elucidated. In the present investigation, we discovered a significant upregulation of the long non-coding RNA GFOD1-AS1(GFOD1-AS1) in the ulcer margin samples of patients with DFU and the HG-induced dysfunction model of human dermal microvascular endothelial cells, attributing its dysregulation to the stabilizing effect of NAT10-mediated ac4C modification, as corroborated by an integrated approach of data mining and experimental validation. Subsequently, a series of in vitro functional analyses showed that ectopic expression of GFOD1-AS1 promoted impaired function of human dermal microvascular endothelial cells. In contrast, knockdown of GFOD1-AS1 significantly alleviated the HG-induced functional impairment in human dermal microvascular endothelial cells, as indicated by the enhanced cell proliferation, migration, and tube formation. Mechanistically, GFOD1-AS1 directly interacts with DNA methyltransferase DNMT1 to block its ubiquitin-proteasome degradation, thereby enhancing the protein stability of DNMT1.This stability elevates DNMT1 protein expression, ultimately inducing HG-induced dysfunction in human dermal microvascular endothelial cells. In summary, our results reveal that GFOD1-AS1 serves as a potential therapeutic target for DFU, and highlight the critical role of the NAT10/GFOD1-AS1/DNMT1 axis in the dysfunction of human dermal microvascular endothelial cells in DFU.

Keywords Diabetic foot ulcer · N4-acetylcytidine modification · GFOD1-AS1 · Human dermal microvascular endothelial cells · DNMT1

Introduction

Diabetic foot ulcer (DFU), a form of foot skin ulceration in diabetic patients arising from long-term hyperglycemia-induced peripheral vascular and neural pathologies, commands significant attention due to its high recurrence rates, amputation incidence, and mortality (Chen et al. 2023; Armstrong et al. 2023). Studies indicate that the risk of developing DFU over a diabetic patient's lifetime can reach up to 34% (Armstrong et al. 2023; Hernandez-Guedes et al. 2023), with DFU being the leading cause of non-traumatic lower limb amputations (Xu et al. 2024). Notably, the 5-year mortality rate among patients who undergo amputations reaches as high as 68%, a figure that surpasses the mortality rates associated with several prevalent cancers, highlighting the critical nature of DFU as a significant health challenge (Zhang et al. 2024). Currently, debridement, antibiotics, application of growth factors, negative pressure wound therapy, hyperbaric oxygen therapy, local oxygen therapy, and skin grafting are common methods used to treat DFU, but

✉ Wenjun Yang
wenjuny88@163.com

[1] Department of Endocrinology and Metabolism, Third Xiangya Hospital of Central South University, Changsha, Hunan 410013, China

[2] Department of Biological Sciences and Biotechnology, College of Life Science and Technology, Jinan University, Guangzhou, Guangdong 510632, China

Published online: 24 May 2025

the recurrence and non-healing nature of DFU remain significant challenges in clinical treatment (Wang et al. 2024; Guo et al. 2024). Therefore, understanding the pathogenesis of DFU and developing effective treatment strategies is crucial for both public health and individual patient care.

Emerging evidence suggests that angiogenesis plays a pivotal role in the wound healing process of DFU, facilitating the delivery of essential nutrients, oxygen, and immune cells to the ulcer site, aiding in the clearance of necrotic tissue, and thereby accelerating DFU wound healing (Rai et al. 2022, 2023). However, hyperglycemia-induced impairment of human dermal microvascular endothelial cells represents a significant impediment to angiogenesis in patients with DFU (Luo et al. 2023a, b; Huang and Huang 2024; Lu et al. 2023). Li's team demonstrated that VEGF-A circular RNA can promote DFU wound healing, characterized by low immunogenicity to promote granulation tissue formation, enhance collagen deposition, and stimulate angiogenesis, which may become a new therapeutic strategy to promote DFU healing (Liu et al. 2024). Therefore, exploring the molecular mechanisms of hyperglycemia-induced dysfunction in human dermal microvascular endothelial cells and identifying novel proangiogenic factors will be crucial for designing more effective DFU therapies.

Accumulating evidence suggests that RNA modifications play a key role in various pathological processes in diabetes. In particular, N4-acetylcytidine (ac4C) is a highly conserved RNA modification in eukaryotes that regulates multiple life cycle stages of mRNA, including processing, decay, and translation, and thus plays a crucial role in a variety of biological processes (Luo et al. 2023a, b). However, it remains unclear whether the ac4C modification plays a role in the impaired angiogenesis associated with DFU. N-acetyltransferase 10 (NAT10) is the only enzyme known to be responsible for the generation of ac4C modification on mRNA in humans (Arango et al. 2018; Wang et al. 2022), which regulates vascular remodeling (Yu et al. 2024) and angiogenesis (Wu et al. 2020) through mRNA ac4C modification. Recent studies have also found that the function of NAT10 is not limited to catalyzing the production of ac4C in mRNA but can also maintain the expression stability of long non-coding RNAs (lncRNAs) by mediating their ac4C modification (Yu et al. 2023). LncRNAs, a class of non-coding RNAs (ncRNAs) longer than 200 nucleotides, participate in the regulation of numerous physiological and pathological processes through epigenetic, transcriptional, and translational control (Herman et al. 2022; Kopp and Mendell 2018), and have been proven to play a key regulatory role in vascular formation of DFU wounds (Yan et al. 2021). LncRNA GAS5 activates the HIF1A/VEGF pathway by binding to TATA-box-binding protein-associated Factor 15 (TAF15), promoting angiogenesis and thus accelerating the healing of DFU wounds (Peng et al. 2021). Nevertheless, the specific function of lncRNAs driven by ac4C modification in the high glucose-induced dysfunction of human dermal microvascular endothelial cells, which results in impaired angiogenesis in DFU, has not been fully elucidated.

In this study, we first systematically identified and screened key lncRNAs closely associated with with the DFU. Our research focused on the regulatory role of GFOD1-AS1 in high glucose-induced functional injury of human dermal microvascular endothelial cells and decipher its specific molecular regulatory mechanism. Furthermore, we investigated the role of ac4C modification in the dysregulation of GFOD1-AS1 in DFU. This insight offers significant guidance for the innovative development of novel drugs and tailored therapeutic strategies for DFU.

Materials and methods

Clinical tissue samples

The study protocol was approved by the ethics committee of the Third Xiangya Hospital of Central South University (No.25033, Date 2025-01-13), and the trial procedures were conducted in accordance with the principles of the Declaration of Helsinki, with each participant providing informed consent after being fully informed about the study. For the experimental group, we procured a total of 10 ulcer margin samples from patients diagnosed with DFU (59 ± 8 years old, 4 man / 6 woman), who exhibited no additional medical complications beyond DFU. In parallel, the control group comprised 10 wound edge samples obtained from patients without DFU (56 ± 10 years old, 5 man / 5 woman), who had skin wounds solely due to trauma and no other underlying diseases. The collected samples were promptly washed in phosphate-buffered saline, subsequently transferred to RNA stabilization solutions, and then preserved at -80 °C for subsequent analysis.

Cell culture

The immortalized human dermal microvascular endothelial cell line (HMEC-1, ZQ0456), purchased from Shanghai Zhong Qiao Xin Zhou Biotechnology Co.,Ltd (Shanghai, China), were cultured in an endothelial cell medium (Shanghai Zhong Qiao Xin Zhou Biotechnology Co.,Ltd, Shanghai, China) supplemented with 5% fetal bovine serum (FBS) at 37 °C in a humidified incubator with 5%CO_2. HMEC-1 cells treated with normal glucose (NG, 5.5 mM glucose) were designated as the control group, and those was exposed to high glucose (HG, 30 mM glucose) were

labeled as the HG group. HMEC-1 cells between passages 15–20 were utilized for all experiments, with regular mycoplasma testing and morphological monitoring to ensure phenotypic consistency.

Cell transfection

The transfection of plasmids and short hairpin RNAs (shRNA) was conducted utilizing Lipofectamine 3000 following the protocol provided by Thermo Fisher Scientific. The GFOD1-AS1, NAT10, DNMT1, and NAT10G641E overexpressing plasmids, and different truncation mutants of GFOD1-AS1 overexpressing plasmids, along with the shRNAs against GFOD1-AS1 and NAT10, were obtained from AIji Biotechnology (GuangZhou, China). The sequences used in this study are summarized in Supplementary Table 1.

Cell proliferation

Cell proliferation was assessed using the Cell Counting Kit-8 (CCK-8) and the 5-ethynyl-2'-deoxyuridine (EdU) assays. For the CCK-8 assay, the designated HMEC-1 cells were treated with the Enhanced Cell Counting Kit (Beyotime, Nanjing, China) according to the manufacturer's instructions, and absorbance was measured at 450 nm using a microplate reader (Tecan, F50) to evaluate cell viability. For the EdU assay, the designated HMEC-1 cells were processed with the BeyoClick™ EdU cell proliferation kit (Beyotime, Nanjing, China) following the manufacturer's protocol, and then stained with Hoechst 33,342 for nuclear visualization. Subsequently, images were captured using an inverted fluorescence microscope (Mshot, MF52), and Image J 1.46r software (National Institutes of Health, Bethesda, Maryland, USA) was utilized to assess cell proliferation by determining the percentage of EdU-positive cells.

Migration assay

The scratch assay was employed to assess the migratory capacity of the indicated cells. Briefly, after HMEC-1 cells were transfected with shRNA or plasmids as described in our previous work, they were seeded in a 6-well plate and subjected to a scratch injury using a sterile 10 µL pipette tip. Cellular migration was monitored by capturing images under an inverted fluorescence microscope (Mshot, MF52) at both the initial (0-hour) and 24-hour time point.

Tube formation assay

The tube formation assay is used to evaluate the angiogenic capacity of the indicated cells. In brief, following the transfection of HMEC-1 cells with shRNA or plasmids as previously detailed, these cells are then inoculated onto a newly prepared endothelial cell medium enriched with 10% FBS and Matrigel (Corning, NY, USA) to observe tube formation. After 24 h of incubation, the cells are captured under an inverted microscope (Mshot, MF52), followed by the quantitative analysis of tube formation parameters with ImageJ 1.46r software (National Institutes of Health, Bethesda, Maryland, USA).

RNA extraction, real-time quantitative PCR (RT-qPCR), and RNA stability assays

In accordance with the manufacturer's protocol, we utilized the PARIS™ Kit (Thermo Fisher Scientific) for the isolation and purification of cytoplasmic and nuclear RNAs. Total RNA extraction from tissues and cells was performed using TRIzol reagent (Takara, Japan). Subsequently, the obtained RNA was reverse transcribed into complementary DNA (cDNA) utilizing the PrimeScript™ RT reagent Kit with gDNA Eraser (Takara, Dalian, china). RT-qPCR was then conducted on the LightCycler®96 system (Roche) using the Benyfast™ SYBR Green qPCR Mix (D7260, Beyotime) following the manufacturer's protocols. Finally, the expression levels were normalized to either glyceraldehyde-3-phosphate dehydrogenase (GAPDH) or 18 S ribosomal RNA (18 S rRNA), and the relative expression levels of the genes were calculated using the $2^{-\Delta\Delta Ct}$ method. For the assessment of RNA stability, the specified HMEC-1 cells were exposed to 5 µM actinomycin D (HY-17559, MEC) at 0, 1, 3, and 5 h post-treatment, and half-life of GFOD1-AS1 was subsequently assessed by measuring GFOD1-AS1 expression levels using RT-qPCR. The primer sequences used for RT-qPCR are shown in Supplementary Table 2.

Protein extraction, western blot, and protein stability/degradation assays

Total proteins were isolated from tissues and cells using pre-chilled radioimmunoprecipitation assay (RIPA) lysis buffer supplemented with protease and phosphatase inhibitors (Solarbio, Beijing, China). Next, the Bicinchoninic Acid assay kit (Beyotime, China) was used to quantify protein concentrations. Equal amounts of protein samples were subjected to sodium dodecyl sulfate-polyacrylamide gel electrophoresis and subsequently transferred to polyvinylidene

fluoride membranes (Millipore, USA). Subsequently, the membranes were blocked with 5% bovine serum albumin and incubated overnight at 4 °C with primary antibodies, followed by incubation with horseradish peroxidase-conjugated secondary antibodies for 2 h at room temperature. Protein bands were visualized using an enhanced chemiluminescence (ECL) reagent (Dingguo Bio, China) on a gel imaging system (GE Healthcare), and densitometric analysis of the bands was conducted using Image J 1.46r software (National Institutes of Health, Bethesda, Maryland, USA). For the assessment of protein stability, the specified cells were exposed to 50 μg/mL CHX (HY-12320, MCE) at 0, 1, 3, and 5 h post-treatment, and the protein half-life subsequently determined through Western blot. In addition, the protein degradation pathway was evaluated by detecting changes in protein expression levels by western blot after the indicated cells were treated with 10 μM MG132 (HY-13259, MCE) or 15 μM CQ (HY-17589 A, MCE). The antibodies used for the study are listed in Supplementary Table 3.

Acetylated RNA immunoprecipitation-qPCR (acRIP-qPCR) assay

The acRIP assay was performed to assess the ac4C modification levels of GFOD1-AS1 utilizing the ac4C Immunoprecipitation Kit from Yun Xu Biotech (Shanghai, China) in accordance with the manufacturer's protocol. Briefly, total RNA extracted using TRIzol reagent (Takara, Dalian, China) was subjected to rapid rRNA removal using the QIAseq FastSelect-rRNA HMR Kit (Qiagen, Shanghai, China) to obtain purified RNA. Following purification, the RNA was randomly sheared into fragments employing an automated ultrasonication device. Subsequently, these fragments were subjected to magnetic immunoprecipitation with the anti-ac4C antibody or an anti-IgG antibody overnight at 4 °C. Ultimately, RNA enriched with ac4C modifications was eluted and purified, and then subjected to RT-qPCR analysis.

LncRNA pull-down assay

The lncRNA pull-down assay was performed according to the method described with suitable modifications. In brief, we transcribed the sense and antisense sequences of GFOD1-AS1, as well as various truncated mutants of GFOD1-AS1 in vitro using the MEGAscript® T7 Transcription Kit (Invitrogen). Subsequently, the transcribed RNA was purified and biotinylated using the Pierce RNA 3' End Desulfurization Biotinylation Kit (Thermo Fisher Scientific). After incubation with cell lysates, the pull-down assay was carried out with the aid of the Pierce Magnetic RNA-Protein Pull-Down Kit (Thermo Fisher Scientific). Ultimately, the captured proteins were subjected to Western blot analysis for validation.

RNA immunoprecipitation-qPCR (RIP-qPCR) assay

The RIP assay was performed using the EZ-Magna RIP™ RNA-Binding Protein Immunoprecipitation Kit (Millipore). Firstly, we pre-incubated the indicated antibody with magnetic beads. Then, the antibody-magnetic bead complex was co-incubated with the cell lysates at 4 °C for an extended period. Following this, the RNA bound to the magnetic beads was eluted and subjected to purification. Ultimately, the enrichment of target genes in the immunoprecipitated RNA-protein complexes was validated using RT-qPCR analysis.

Ubiquitination assay

The indicated HMEC-1 cells were treated with 10 μM MG132 (HY-13259, MCE) for 12 h, after which these cells were lysed using a lysis buffer containing protease and phosphatase inhibitors to extract the total protein. Subsequently, we conducted immunoprecipitation using the Pierce™ Co-Immunoprecipitation Kit (Thermo Fisher Scientific) in conjunction with an anti-DNMT1 antibody (ab19905, Abcam) in accordance with the manufacturer's guidelines. Post-immunoprecipitation, the precipitates were meticulously collected by centrifugation and extensively washed to eliminate any unbound proteins. Finally, the precipitates enriched with DNMT1 protein complexes were subjected to Western blot analysis using a specific anti-ubiquitin antibody (Ab134953, Abcam) to evaluate the ubiquitination status of DNMT1.

Data source and statistical analysis

The GSE80178 dataset was obtained from the Gene Expression Omnibus (GEO) database (https://www.ncbi.nlm.nih.gov/geo/query/acc.cgi?acc=GSE80178), which includes samples from the ulcer margins of six DFU patients and six normal skin samples from non-DFU individuals. Employing the R programming language along with specialized bioinformatics packages, we processed and analyzed this dataset to extract the lncRNA expression profiles. To identify differentially expressed lncRNAs between the two groups, we applied the criteria of $|\log FC| > 1.0$ and $P < 0.01$. Coding Potential Calculator 2 (CPC2.0) online databases (https://cpc2.gao-lab.org/) was used to analysis the coding potential of GFOD1-AS1. The PACES online database (http://www.rnanut.net/paces/) was leveraged to identify and map the ac4C modification motifs present on the GFOD1-AS1 transcript. Furthermore, the catRAPID online database

(http://s.tartaglialab.com/page/catrapid_group) and RPISeq online database (http://pridb.gdcb.iastate.edu/RPISeq/) were utilized to forecast the proteins that may interact with GFOD1-AS1, and the specific sequence of DNMT1 binding on GFOD1-AS1.

For quantitative analyses, each experiment was performed in triplicate to ensure reliability. Data are presented as the mean values ± standard deviations (SD). All data processing and statistical analyses were conducted using GraphPad Prism Software (GraphPad Inc., La Jolla, CA, USA). To compare groups, we employed a two-tailed Student's t-test for comparing two groups and a one-way ANOVA with Tukey's multiple comparison test for analyzing multiple groups. Statistical significance was set at a threshold of $P < 0.05$.

Results

NAT10-mediated ac4C modification drives the aberrant upregulation of GFOD1-AS1 in ulcer margin tissues from patients with diabetic foot ulcers (DFU) and in high glucose (HG)-treated human dermal microvascular endothelial cells

By differential analysis of the whole-genome lncRNA expression profiles (|logFC| > 1.0 and P-value < 0.01) from the GSE80178 dataset comprising ulcer margin samples from six DFU patients and normal skin samples from six non-DFU individuals, we screened a series of lncRNAs that were dysregulated in the ulcer margin tissues of DFU patients, of which 18 lncRNAs were significantly up-regulated (Fig. 1A and Supplementary Table 4). To ensure unbiased validation and avoid biased selection of known or highly specialized lncRNAs, a systematic randomization method was used to randomly selected five lncRNAs (HIF1A-AS2, LINC00520, LINC00462, GFOD1-AS1, and FAM83C-AS1) from the 18 up-regulated lncRNAs to validate their expression levels in clinical samples. The RT-qPCR analysis revealed that LINC00520, HIF1A-AS2, and GFOD1-AS1 were significantly elevated in the ulcer margin tissues of patients with DFU, with GFOD1-AS1 demonstrating the most pronounced difference (Fig. 1B). Consequently, GFOD1-AS1 was chosen for further investigation. Subsequently, we treated HMEC-1 cells with high glucose (HG, 30 mM glucose) to mimic human dermal microvascular endothelial cell dysfunction in DFU. We then monitored the expression changes of GFOD1-AS1 using RT-qPCR, and discovered a significant upregulation of GFOD1-AS1 in the HG-induced dysfunction of HMEC-1 cells (Fig. 1C), which corroborated the expression patterns observed in clinical samples. These data illustrate that GFOD1-AS1 is significantly upregulated in ulcer edge samples from DFU patients and in human dermal microvascular endothelial cells under high glucose conditions. Although recent studies have reported that lncRNAs are capable of encoding peptides or proteins (Zhang 2024; Yi et al. 2024), our analysis using the CPC2.0 online database has revealed that GFOD1-AS1 lacks the potential for protein coding (Supplementary Fig. 1A). Furthermore, we investigated the intracellular localization of GFOD1-AS1 by performing RT-qPCR after isolating RNA from the cytoplasm and nucleus. Our findings revealed that GFOD1-AS1 is present in both the cytoplasmic and nuclear fractions, with a predominant localization in the nucleus (Supplementary Fig. 1B).

To further investigate the underlying mechanisms of the abnormal upregulation of GFOD1-AS1 in the ulcer margin tissues of patients with DFU, we predicted the presence of ac4C modification on GFOD1-AS1 transcripts using the PACES online tool (Supplementary Fig. 1C). Subsequently, we employed acRIP-qPCR assay to detect the ac4C modification levels of GFOD1-AS1 in clinical specimens. Our analysis revealed a substantial increase in ac4C modification levels of GFOD1-AS1 in the ulcer margin tissues of DFU patients, which was positively correlated with the expression levels of GFOD1-AS1 (Fig. 1D). These data suggest that ac4C modification may contribute to the promotion of GFOD1-AS1 expression in the ulcer margin skin tissues of patients with DFU. NAT10, identified as the sole ac4C "writer" protein, acts as an RNA acetyltransferase that catalyzes ATP-dependent acetylation, specifically introducing ac4C modifications into mRNAs and non-coding RNAs. Consequently, we employed RT-qPCR to examine NAT10 expression levels in clinical samples and HMEC-1 cells exposed to HG. RT-qPCR results showed a significant upregulation of NAT10 mRNA in the ulcer margin skin tissues of DFU patients and in HG-treated HMEC-1 cells (Fig. 1E). Next, we engineered shRNA constructs specifically targeting NAT10 and transfected them into HMEC-1 cells, subsequently assessing transfection efficiency using RT-qPCR. The results showed that all three shNAT10 had significant interference effects, with shNAT10#1 demonstrating the best interference effect (Figs. 1F), which was used for subsequent studies. Interestingly, our findings revealed that the suppression of NAT10 substantially decreased both the transcript expression and ac4C modification levels of GFOD1-AS1 in HG-induced HMEC-1 cells (Figs. 1G and Supplementary Fig. 1D). Previous studies have reported that a mutation of the conserved glycine residue to glutamic acid (G641E) in NAT10 leads to a loss of its acetylation function (Gong et al. 2024). HMEC-1 cells were transfected with the FLAG-tagged catalytically inactive mutant of NAT10 (G641E) and its wild type, and then Western blot were conducted using an anti-flag antibody. The results showed

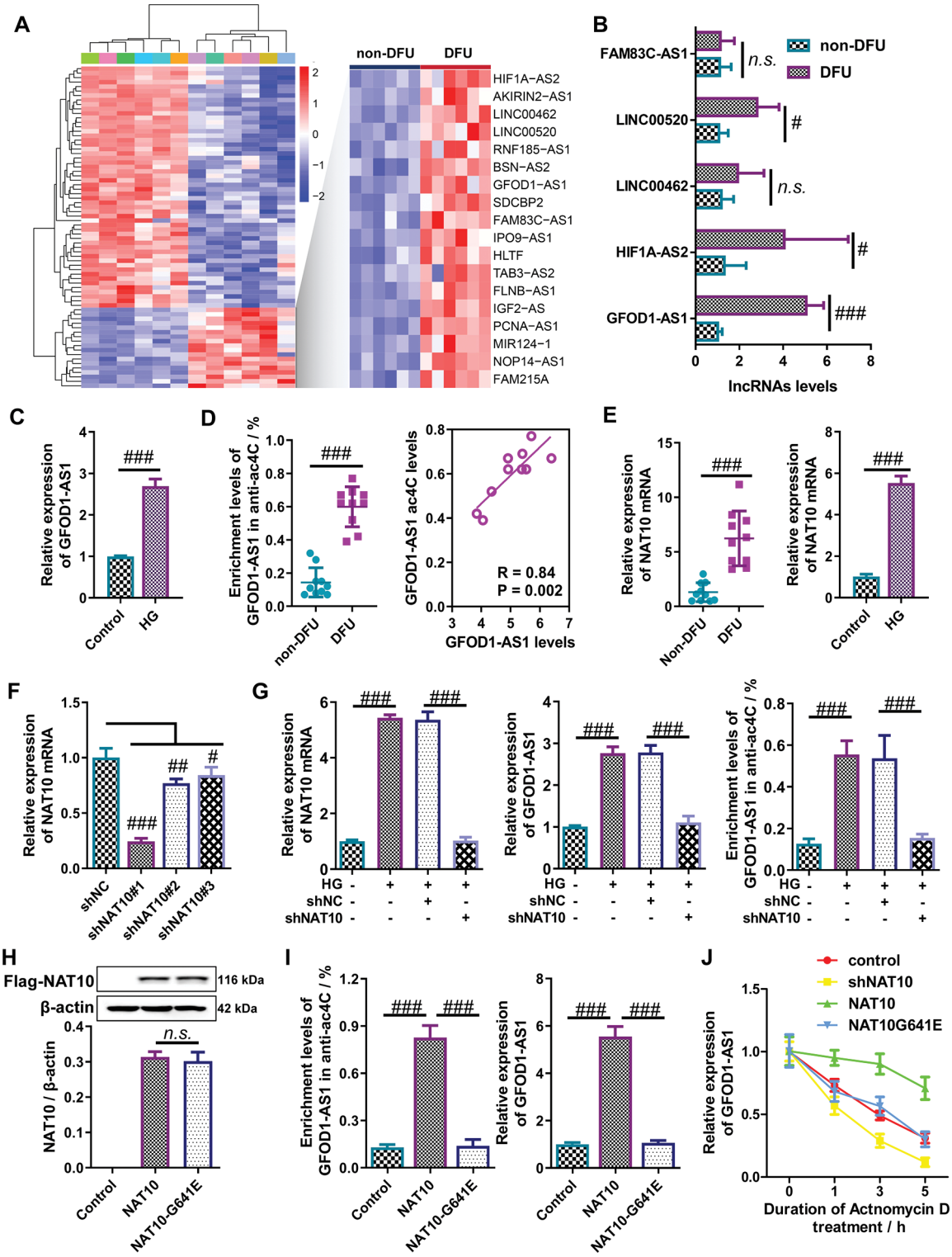

no significant difference in NAT10 protein levels between HMEC-1 cells transfected with NAT10-G641E and those with the wild-type NAT10 (Fig. 1H). Further analysis using RT-qPCR and acRIP-qPCR assays demonstrated that the overexpression of wild-type NAT10 significantly elevated both the transcript levels and ac4C modification levels of GFOD1-AS1, but overexpression of NAT10-G641E exhibited no significant effect on these levels (Fig. 1I). Finally, RNA stability assay revealed that NAT10 knockdown accelerated the degradation of GFOD1-AS1, and overexpression of NAT10 decelerated it, yet the overexpression of the catalytically inactive NAT10-G641E mutant exhibited no effect

Fig. 1 NAT10-mediated ac4C modification increases GFOD1-AS1 stability in diabetic foot ulcer (DFU). (**A**) Analysis of the GSE80178 dataset using a heatmap disclosed distinct long non-coding RNA (lncRNA) expression patterns, with significant differential expression (|logFC| > 1.0 and $P<0.01$) observed in ulcer margin samples from six individuals with DFU and normal skin samples from six non-DFU patients. Notably, 18 lncRNAs were markedly up-regulated specifically in ulcer margin samples from patients with DFU. (**B**) Reverse transcription quantitative polymerase chain reaction (RT-qPCR) was employed to quantify the expression levels of long non-coding RNAs HIF1A-AS2, LINC00520, LINC00462, GFOD1-AS1, and FAM83C-AS1 in ulcer margin samples from ten individuals with DFU and wound margin normal skin samples from ten non-DFU patients. (**C**) RT-qPCR was utilized to assess the expression levels of GFOD1-AS1 in human dermal microvascular endothelial cells (HMEC-1 cells) under conditions of high glucose (HG) treatment and normal glucose control. (**D**) The enrichment of acetylation at lysine 4 (ac4C) modification on GFOD1-AS1 was determined using anti-acetyl-lysine RNA immunoprecipitation (acRIP) in ulcer margin samples from ten individuals with DFU and wound margin normal skin samples from ten non-DFU patients, and Pearson correlation coefficient analysis revealed a significant positive correlation between the transcript levels of GFOD1-AS1 and its ac4C modification levels in ulcer margin samples from patients with DFU. (**E**) RT-qPCR was employed to measure NAT10 expression levels in ulcer margin samples from ten individuals with DFU and wound margin normal skin samples from ten non-DFU patients, as well as HMEC-1 cells under conditions of HG treatment and normal glucose control. (**F**) RT-qPCR was utilized to assess GFOD1-AS1 expression levels following transfection of HMEC-1 cells with shNC or shNAT10. (**G**) acRIP-qPCR and RT-qPCR were employed to evaluate the enrichment of GFOD1-AS1 with the ac4C antibody and the expression levels of GFOD1-AS1 and NAT10 in HMEC-1 cells under HG conditions. (**H**) Western blot analysis revealed no significant difference in NAT10 protein expression levels between HMEC-1 cells overexpressing NAT10 and those overexpressing the NAT10-G641E. (**I**) acRIP-qPCR and RT-qPCR were used to assess the enrichment of GFOD1-AS1 with the ac4C antibody and to determine GFOD1-AS1 expression levels in HMEC-1 cells overexpressing either NAT10 or the NAT10-G641E. (**J**) RNA stability assays were conducted to evaluate the impact of NAT10 on the degradation of GFOD1-AS1. DFU, diabetic foot ulcers; HG, high glucose; shNC, negative control short hairpin RNA vector; shNAT10, NAT10 short hairpin RNA vector; NAT10, NAT10 overexpression vector; NAT10G641E, NAT10G641E overexpression vector. $N=3$, $^{n.s.}p>0.05$, $^{\#}p<0.05$, $^{\#\#}p<0.01$, and $^{\#\#\#}p<0.001$

on GFOD1-AS1 stability (Fig. 1J). Collectively, these data suggest that NAT10-mediated ac4C modification enhances GFOD1-AS1 stability, leading to the aberrant upregulation of GFOD1-AS1.

Knockdown of GFOD1-AS1 enhances the proliferation, migration, and tube formation of human dermal microvascular endothelial cells under high-glucose

To elucidate the role of GFOD1-AS1 in HG-induced dysfunction of human dermal microvascular endothelial cells, shRNA constructs specifically targeting GFOD1-AS1 were transfected into HMEC-1 cells. The results from RT-qPCR showed that all three shGFOD1-AS1 had significant interference effects, with shGFOD1-AS1#1 demonstrating the best interference effect (Fig. 2A), which was used for subsequent studies. Subsequently, HMEC-1 cells with and without GFOD1-AS1 knockdown were subjected to HG treatment for 24-hour to mimic the human dermal vascular endothelial cell dysfunction in DFU. Our findings revealed that the knockdown of GFOD1-AS1 in HMEC-1 cells significantly abrogated the HG-induced upregulation of GFOD1-AS1 expression (Fig. 2B). CCK-8 and EdU staining assays revealed that HG significantly suppressed the proliferation of HMEC-1 cells, and this inhibitory effect was substantially reversed by the knockdown of GFOD1-AS1 (Fig. 2C and D, and 2E). Scratch assay results showed that knockdown of GFOD1-AS1 could largely rescue the inhibitory effect of HG on HMEC-1 cells migration (Fig. 2F and G). Tube formation assay results indicated that knockdown of GFOD1-AS1 could eliminate the inhibitory effects of HG on tube formation of HMEC-1 cells, characterized by a significant increase in number meshes, number segments, number branches, and total branching length (Fig. 2H and I, and Supplementary Fig. 2). Additionally, Western blot analysis was utilized to assess the tube-forming ability of HMEC-1 cells by quantifying the protein expression levels of angiogenesis markers, including VEGF, HIF-1α, and CD31. The results revealed that HG significantly reduced the protein expression of VEGF, HIF-1α, and CD31 in HMEC-1 cells, and this suppressive effect was substantially mitigated by the knockdown of GFOD1-AS1 (Fig. 2J), implying that GFOD1-AS1 knockdown may counteract the inhibitory impact of HG on angiogenesis. Ultimately, we assessed the functional consequences of GFOD1-AS1 overexpression in human dermal microvascular endothelial cells. The results from RT-qPCR indicated that transfection of HMEC-1 cells with the GFOD1-AS1 overexpression plasmid significantly increased the expression of GFOD1-AS1 (Fig. 3A), confirming the success of the transfection. EdU staining assay demonstrated that overexpression of GFOD1-AS1 significantly inhibited cell proliferation in HMEC-1 cells (Fig. 3B). Scratch assays confirmed that GFOD1-AS1 overexpression markedly reduced cell migration in HMEC-1 cells (Fig. 3C). Furthermore, Western blot analysis revealed that GFOD1-AS1 overexpression substantially inhibited the protein expression of angiogenic markers (VEGF, HIF-1α, and CD31) in HMEC-1 cells (Fig. 3D), suggesting that elevated GFOD1-AS1 levels can impede angiogenesis. The collective data indicate that GFOD1-AS1 plays a crucial role in HG-induced dysfunction of human dermal microvascular endothelial cells, and knockdown of GFOD1-AS1 can ameliorate the HG-induced dysfunction of human dermal microvascular endothelial cells.

GFOD1-AS1 increases DNMT1 protein levels by directly interacting with DNMT1 to block its ubiquitin degradation

To clarify the regulatory mechanism of GFOD1-AS1 in high glucose-induced functional injury of human dermal microvascular endothelial cells, we initially investigated whether GFOD1-AS1 acts as a competing endogenous RNA (ceRNA). RIP-qPCR assay was performed to investigate the potential interaction between GFOD1-AS1 and Argonaute-2 (Ago2), an integral component of the RNA-induced silencing complex (RISC). The result from RIP-qPCR revealed that GFOD1-AS1 was undetected in the Ago2-associated cellular fraction, thereby excluding the possibility of GFOD1-AS1 functioning as a ceRNA (Supplementary Fig. 3A). A multitude of studies have demonstrated that interactions with RNA-binding proteins are a prevalent mechanism by which lncRNAs modulate downstream biological factors. Consequently, we employed the catRAPID online prediction platform (http://s.tartaglialab.com/page/catrapid_group) to forecast potential protein interactions with GFOD1-AS1. Our analysis revealed that DNA methyltransferase 1 (DNMT1) is among the proteins that interact with GFOD1-AS1 (Fig. 4A). Further analysis using RPISeq online prediction platform (http://pridb.gdcb.iastate.edu/RPISeq/) revealed a score of 0.89 for the interaction between DNMT1 and GFOD1-AS1, further suggesting their interaction. Subsequently, we conducted RNA pull-down assays using probes specific to both the sense and antisense strands of GFOD1-AS1, followed by Western blot analysis. Our findings showed that DNMT1 was selectively enriched in the complexes pulled down by the sense strand of GFOD1-AS1, not the antisense strand of GFOD1-AS1(Fig. 4B), suggesting a specific interaction between DNMT1 and GFOD1-AS1. Additionally, we conducted RIP assays using anti-IgG and anti-DNMT1 antibodies in HMEC-1 cells with or without HG treatment, followed by RT-qPCR analysis. The results demonstrated that DNMT1 interacted with GFOD1-AS1, and that this interaction is significantly enhanced by HG exposure (Fig. 4C). Based on the catRAPID-identified sequence potentially binding DNMT1 on GFOD1-AS1, we constructed sense and antisense GFOD1-AS1, along with several truncated mutants (Fig. 4D). We then performed RNA pull-down assay in conjunction with Western blot analysis to evaluate the binding affinity of DNMT1 for these sequences on GFOD1-AS1. The results indicated that DNMT1 was specifically detected in the pull-down fractions corresponding to the sense GFOD1-AS1 and its Δ3 and Δ4 truncated mutants, but not in those corresponding to the antisense GFOD1-AS1 and its Δ5 and Δ6 truncated mutants (Fig. 4E), suggesting that the sequence 1172nt-1248nt on GFOD1-AS1 interacts with DNMT1. In summary, GFOD1-AS1 engages in direct interactions with DNMT1, pinpointing the nucleotide sequence between positions 1172 and 1248 on GFOD1-AS1 as the specific binding site.

In our ongoing analysis of the regulatory interplay between GFOD1-AS1 and DNMT1, we observed that DNMT1 expression levels were significantly elevated in the ulcer margin tissues of patients with DFU and in HG-treated HMEC-1 cells (Supplementary Fig. 3B and Fig. 4F). Interestingly, the knockdown of GFOD1-AS1 substantially suppressed HG-induced DNMT1 protein expression in HMEC-1 cells, without impacting DNMT1 mRNA levels (Fig. 4F), suggesting that GFOD1-AS1 regulates DNMT1 expression at the post-translational level. Consequently, we performed protein degradation experiments in HMEC-1 cells using50 μg/mL CHX (the protein synthesis inhibitor). Western blot analysis revealed that knockdown of GFOD1-AS1 significantly reduced the half-life of DNMT1 protein in HMEC-1 cells (Fig. 4G). These data indicated that knockdown of GFOD1-AS1 markedly promoted the degradation of DNMT1 protein.

Ubiquitination, a post-translational modification that involves the conjugation of ubiquitin to target proteins, is pivotal in the regulation of numerous biological processes (Wang and Maldonado 2006; Zhong et al. 2022). Current evidence indicates that proteins modified by ubiquitination are primarily degraded through the ubiquitin-proteasome system and the autophagy-lysosome system (Cui et al. 2024). Thus, we treated the specified HMEC-1 cells with MG132 (an inhibitor of the ubiquitin-proteasome pathway) or CQ (an inhibitor of the autophagy-lysosome pathway). Western blot analysis revealed that MG132, but not CQ, significantly mitigated the degradation of DNMT1 protein triggered by GFOD1-AS1 knockdown (Fig. 4H), suggesting that the knockdown of GFOD1-AS1 promotes DNMT1 protein degradation primarily through the ubiquitin-proteasome system. Subsequently, DNMT1 ubiquitination levels were evaluated by Western blot after co-immunoprecipitating the specified HMEC-1 cells with an anti-DNMT1 antibody. The results revealed that knockdown of GFOD1-AS1 significantly enhanced the ubiquitination levels of DNMT1 protein in HMEC-1 cells, and this promotion could be abolished by overexpression of GFOD1-AS1 (Fig. 4I), suggesting that knockdown of GFOD1-AS1 facilitates DNMT1 protein ubiquitination levels in HMEC-1 cells. Finally, Western blot analysis showed that overexpressing GFOD1-AS1 increased DNMT1 protein levels in HMEC-1 cells with GFOD1-AS1 knockdown, whereas overexpression of the truncated mutant GFOD1-AS1-△6 had no effect on DNMT1 expression (Fig. 4J). Collectively, these data conclude that GFOD1-AS1 enhances the stability of DNMT1 by directly binding to DNMT1 and inhibiting the

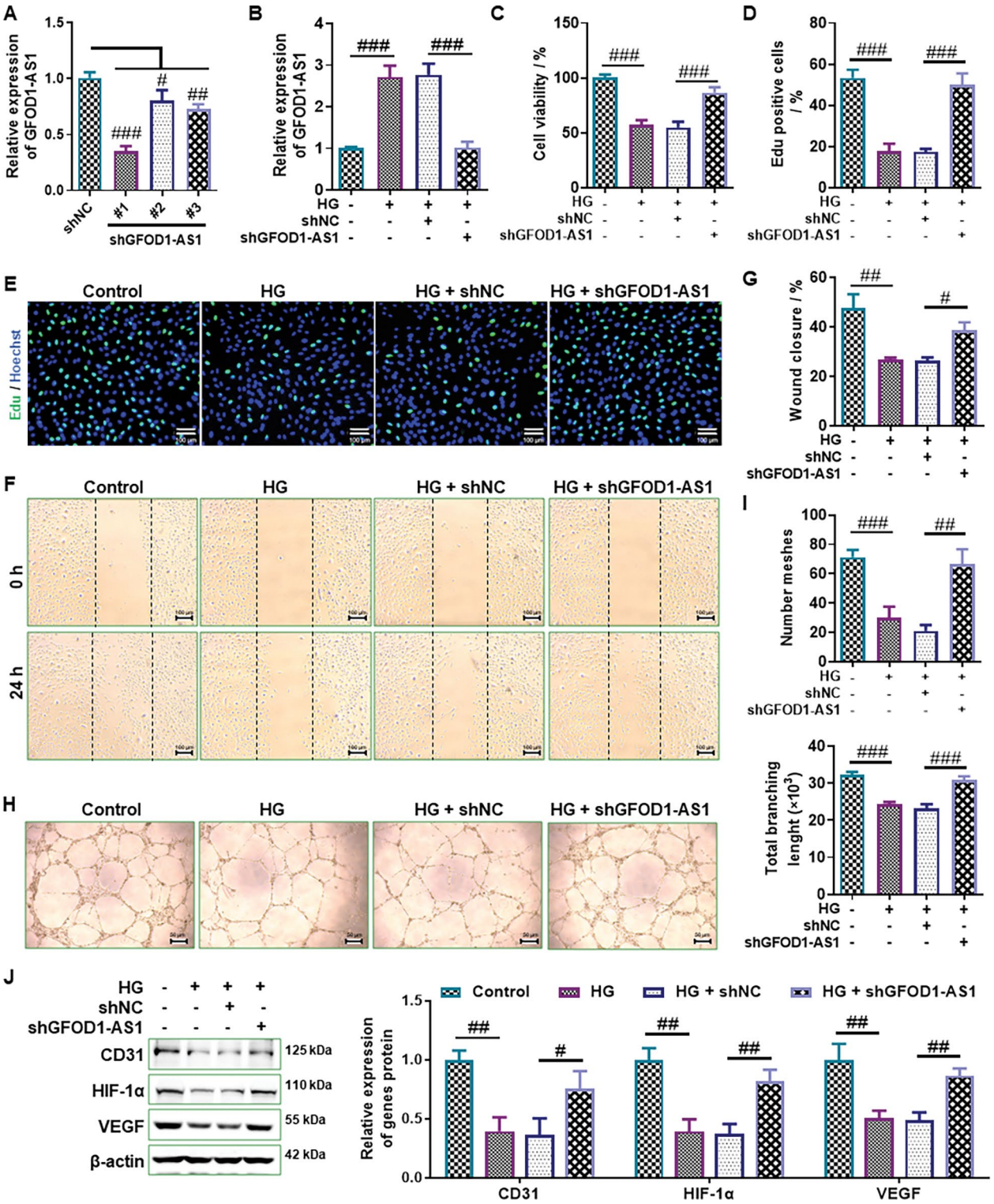

Fig. 2 Knockdown of GFOD1-AS1 enhances the proliferation, migration, and tube formation of human dermal microvascular endothelial cells under high-glucose. (**A**) RT-qPCR was used to determine the expression levels of GFOD1-AS1 in HMEC-1 cells following transfection with three different shGFOD1-AS1 or shNC, thereby assessing the efficiency of transfection. (**B**) RT-qPCR was conducted to measure GFOD1-AS1 expression levels in the specified HMEC-1 cells. (**C**-**E**) The CCK-8 and EdU assays were used to measure the proliferation ability of the indicated HMEC-1 cells. Scale bar = 100 μm. (**F**-**G**) The wound healing assay was applied to detect the migration of the indicated HMEC-1 cells. Scale bar = 100 μm. (**H**-**I**) The tube formation assay was utilized to evaluate the angiogenic tube formation capacity of the specified HMEC-1 cells. Scale bar = 50 μm. (**J**) Western blot analysis was conducted to assess the protein expression levels of angiogenic markers, including VEGF, HIF-1α, and CD31, in the indicated HMEC-1 cells. HG, high glucose; shNC, negative control short hairpin RNA vector; shGFOD1-AS1, GFOD1-AS1 short hairpin RNA vector. $N = 3 \sim 5$, $^{\#}p < 0.05$, $^{\#\#}p < 0.01$, and $^{\#\#\#}p < 0.001$

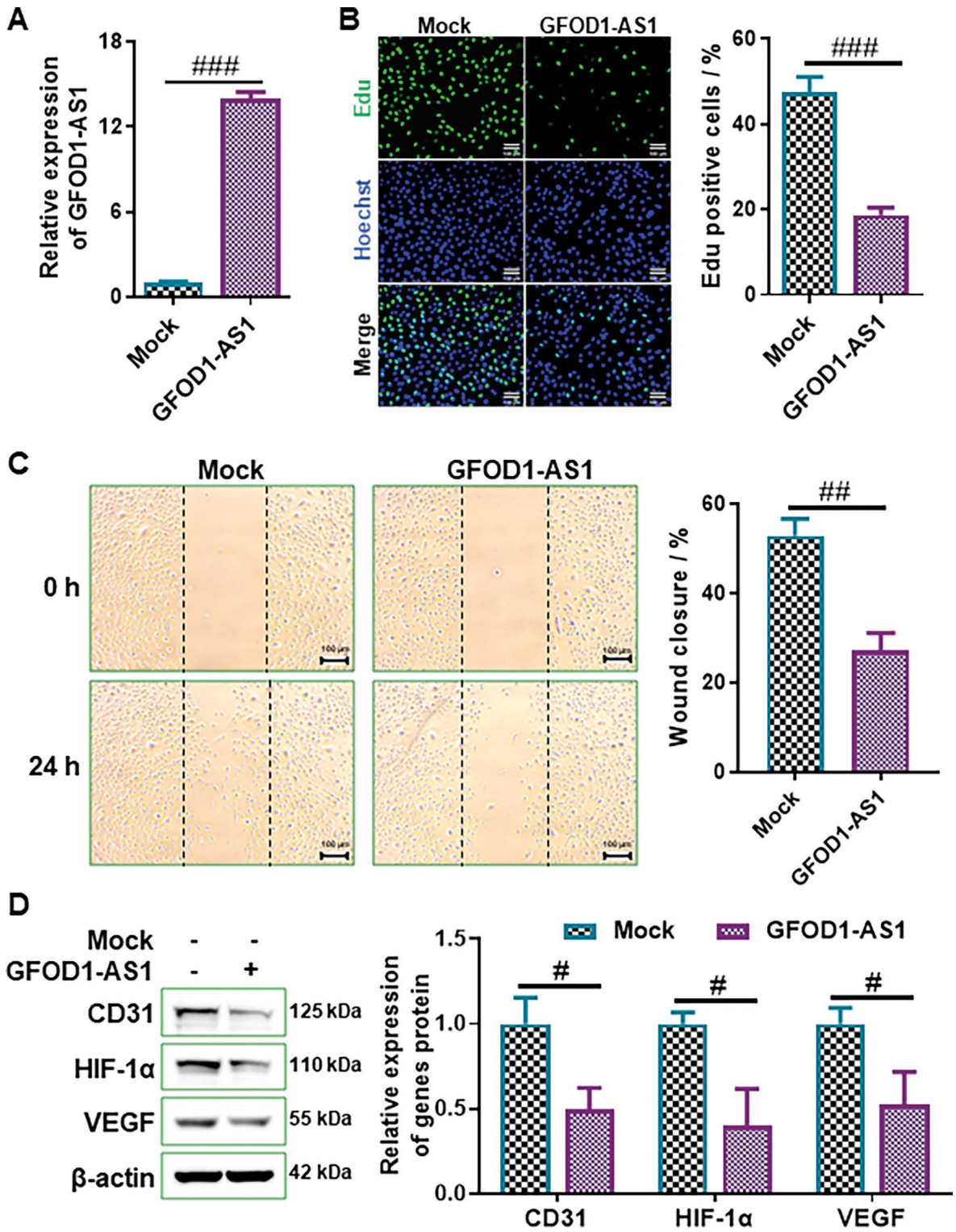

Fig. 3 Elevated levels of GFOD1-AS1 suppress the proliferation, migration, and tube formation capabilities of human dermal microvascular endothelial cells. (**A**) RT-qPCR was used to determine the expression levels of GFOD1-AS1 in HMEC-1 cells following transfection with GFOD1-AS1 or mock, thereby assessing the efficiency of transfection. (**B**) The EdU assay was used to measure the proliferation ability of HMEC-1 cells with or without GFOD1-AS1 overexpression. Scale bar = 100 μm. (**C**) The wound healing assay was employed to assess the migratory capability of HMEC-1 cells with or without GFOD1-AS1 overexpression. Scale bar = 100 μm. (**D**) Western blot analysis was conducted to assess the protein expression levels of angiogenic markers (VEGF, HIF-1α, and CD31) in HMEC-1 cells with or without GFOD1-AS1 overexpression. Mock, negative control vector; GFOD1-AS1, GFOD1-AS1 expressed vector. $N = 3$, $^{\#}p < 0.05$, $^{\#\#}p < 0.01$, and $^{\#\#\#}p < 0.001$

degradation of DNMT1 protein mediated by the ubiquitin-proteasome pathway.

Knockdown of GFOD1-AS1 ameliorates HG-induced functional impairments in human dermal microvascular endothelial cells by downregulating DNMT1 expression

To determine whether DNMT1 is an effector of GFOD1-AS1 in DFU, we constructed HMEC-1 cells overexpressing DNMT1 (Supplementary Fig. 4A) and performed rescue experiments in the indicated HMEC-1 cells with HG-induced functional impairment, with comprehensive comparison between high glucose and control groups provided in Figs. 1 and 2. Western blot analysis demonstrated that transfection of HMEC-1 cells with DNMT1 expression plasmids not only enhanced HG-induced DNMT1 expression but also negated the suppressive effect of GFOD1-AS1 knockdown on HG-induced DNMT1 expression (Supplementary Fig. 4B). Subsequently, EdU assay revealed that overexpression of DNMT1 significantly aggravated the inhibitory effect of HG on cell proliferation and also counteracted the ameliorative effect of GFOD1-AS1 knockdown on HG-induced proliferation inhibition (Fig. 5A and B). Scratch assay results evaluating cell migration capacity indicated that overexpression of DNMT1 significantly intensified the inhibitory impact of HG on cell migration and also negated the beneficial effects of GFOD1-AS1 knockdown in mitigating HG-induced migration inhibition (Fig. 5C and D). Tube formation assay data, which evaluate angiogenic potential, demonstrated that overexpression of DNMT1 significantly exacerbated the inhibitory effect of HG on tube formation and also abrogated the beneficial impact of GFOD1-AS1 knockdown on alleviating HG-induced inhibition of tube formation (Fig. 5E and F, and Supplementary Fig. 4C). Furthermore, Western blot analysis of angiogenic markers (VEGF, HIF-1α, and CD31) revealed that overexpression of DNMT1 markedly intensified the suppressive impact of HG on the expression levels of these proteins and neutralized the influence of GFOD1-AS1 knockdown on their expression profiles under HG conditions (Fig. 5G). Collectively, these findings underscore the overexpression of DNMT1 inhibits the biological function of human dermal microvascular endothelial cells in HG conditions, whereas the knockdown of GFOD1-AS1 enhances the biological functions of these cells under high-glucose conditions by downregulating DNMT1.

Discussion

Existing studies have confirmed that the hyperglycemic microenvironment in DFU contributes to delayed wound repair by inducing dysfunction in dermal microvascular endothelial cells. Nevertheless, the central molecular regulatory network underlying DFU pathogenesis remains elusive. This study aims to clarify the pathogenesis of high glucose-induced dermal microvascular endothelial cell dysfunction and provide potential therapeutic targets for the clinical management of DFU.

Although lncRNAs play a significant role in various diseases, including DFU (Yan et al. 2021; Architha et al. 2024; Li et al. 2020), the underlying regulatory mechanisms are not well understood. Emerging evidence underscores the pivotal role of ac4C modification in the regulation of lncRNA expression (Yu et al. 2023; Gong et al. 2024; Yan et al. 2023). Nevertheless, ac4C modification driving lncRNA dysregulation in DFU has yet to be documented. In this study, we report for the first time that a substantial increase in ac4C modification levels of GFOD1-AS1 in the ulcer margin tissues of DFU patients was positively correlated with the expression levels of GFOD1-AS1, suggesting that ac4C modification may contribute to the promotion of GFOD1-AS1 expression in the ulcer margin skin tissues of patients with DFU. NAT10 is the only known AC4C-modified writer, which has been proved to be involved in the occurrence and development of a variety of human diseases. Recent studies have shown that NAT10 can not only mediate mRNA ac4C modification to maintain mRNA stability and translation, but also promote lncRNA ac4C modification to enhance lncRNA stability. For example, NAT10 enhances the stability of lncRNA SIMALR in nasopharyngeal carcinoma (Gong et al. 2024), lncRNA CTC-490G23.2 stability (Yu et al. 2023) in cancer metastasis, and lncRNA PAN stability in the context of the kaposi's sarcoma-associated herpesvirus (KSHV) infection (Yan et al. 2023) by mediating ac4C modification. Consistent with previous research, our findings also demonstrated that the abnormal upregulation of GFOD1-AS1 in DFU is attributed to NAT10-mediated ac4C modification enhancing GFOD1-AS1 stabilization. Most notably, our findings reveal that GFOD1-AS1 directly interacts with DNMT1, preventing its ubiquitin-mediated degradation and preserving DNMT1 protein stability, which in turn exacerbates HG-induced dysfunction in human dermal microvascular endothelial cells.

The swift evolution in the fields of proteomics and epigenetics has facilitated the discovery of numerous RNA-binding proteins (RBPs), which in turn has propelled research into the intricate interplay between lncRNAs and RBPs (Bian et al. 2019; Yang et al. 2019). Kang et al. reported that lncRNA MIR210HG interacts with DNMT1, recruiting

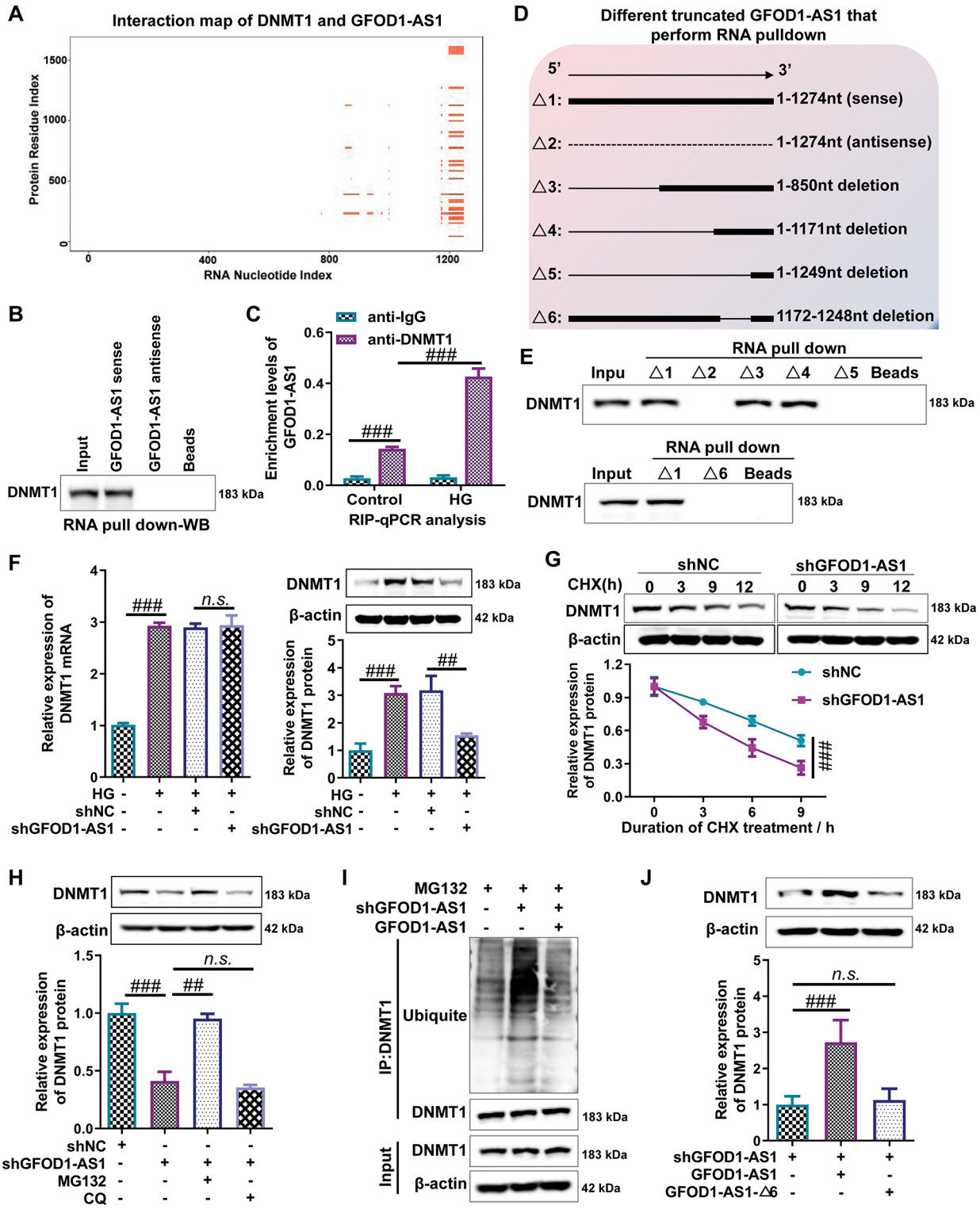

DNMT1 to the CACNA2D2 gene promoter to activate its methylation, thereby suppressing the transcriptional expression of CACNA2D2, leading to the proliferation and invasion of non-small cell lung cancer (Kang et al. 2019). Wang et al. found that lncRNA TINCR directly interacts with DNMT1, promoting the methylation of the miR-503-5p gene, thus inhibiting the transcriptional expression of miR-503-5p, resulting in the proliferation and tumorigenesis of breast cancer cells (Wang et al. 2021). Fu et al. reported that LINC01435 changed the subcellular localization of the transcription factor Yin Yang 1 (YY1) and cinteracted with YY1 to upregulate the expression of histone deacetylases8

Fig. 4 GFOD1-AS1 interacts with DNMT1 to block the degradation of DNMT1 mediated by ubiquitin-proteasome pathway and up-regulate the expression of DNMT1. (**A**) The CatRAPID online platform was utilized to predict interactions between DNMT1 and GFOD1-AS1. (**B**) Western blot analysis confirmed the enrichment of DNMT1 in the fractions specifically pulled down by GFOD1-AS. (**C**) RNA immunoprecipitation (RIP) assays were performed on HMIC-1 cells from the HG and control groups using anti-IgG antibody (negative control) and anti-DNMT1 antibody, and the enrichment of GFOD1-AS1 in the precipitates was quantified by RT-qPCR. RIP-qPCR results confirmed that the DNMT1-directed antibody was capable of precipitating GFOD1-AS1. (**D**) The schematic diagram illustrates the full-length, antisense, and different truncated fragments of GFOD1-AS1. (**E**) RNA pull down-western blot analysis revealed that the truncated fragment #6 of GFOD1-AS1 was indispensable for the interaction with DNMT1. (**F**) RT-qPCR and Western blot analysis were employed to determine the relative mRNA and protein levels of DNMT1 in indicated HMEC-1 cells. (**G**) HMEC-1 cells transfected with shGFOD1-AS1 or shNC were treated with 50 μg/mL cycloheximide (CHX) for specified time periods, after which DNMT1 protein levels were assessed using Western blot analysis. (**H**) HMEC-1 cells transfected with shGFOD1-AS1 or shNC were treated with 10 μM MG132 or 15 μM chloroquine (CQ) for specified time periods, and then DNMT1 protein levels was detected by Western blot analysis. (**I**) HMEC-1 cells transfected with shGFOD1-AS1 or overexpressing GFOD1-AS1 were treated with 10 μM MG132 for 10 h, and then the ubiquitination level of DNMT1 was evaluated using co-immunoprecipitation (Co-IP) followed by Western blot analysis. (**J**) Western blot analysis was performed to detect the expression of DNMT1 protein in HMEC-1 cells after knockdown of GFOD1-AS1, followed by re-expression of GFOD1-AS1 or GFOD1-AS1-△6. HG, high glucose; DNMT1, DNMT1 overexpression vector; shGFOD1-AS1, GFOD1-AS1 short hairpin RNA vector; GFOD1-AS1, GFOD1-AS1overexpression vector; △1, Full-length vector of GFOD1-AS1; △2, Antisense vector of GFOD1-AS1; △3, A truncated GFOD1-AS1 containing 851-1274nt; △4, A truncated GFOD1-AS1 containing 1172-1274nt; △5, A truncated GFOD1-AS1 containing 1248-1274nt; △6, A truncated GFOD1-AS1 deletion of 1172-1248nt (GFOD1-AS1-△6). $N=3$, $^{n.s}p>0.05$, $^{\#\#}p<0.01$, and $^{\#\#\#}p<0.001$

(HDAC8), thereby inhibiting the tube formation and migration of human endothelial cells, and consequently exacerbating DFU (Fu et al. 2022). In concordance with existing literature, our research also demonstrates that GFOD1-AS1 exerts its function in DFU by engaging directly with the DNMT1 protein, thereby negating the ceRNA mechanism as the primary mediator of its action.

DNMT1, a crucial gene in mammalian DNA methylation, encodes a large and complex enzyme that contributes to the multitude of regulatory capabilities. Previous studies have demonstrated that high glucose-driven overexpression of DNMT1 can lead to microvascular endothelial dysfunction, and inhibition of DNMT1 can ameliorate high glucose-induced impairment of angiogenesis and accelerate the healing of diabetic wounds (Zhao et al. 2021; Xue et al. 2022). These findings underscores the pivotal role of DNMT1 in the pathogenesis of diabetic vascular complications, suggesting that DNMT1 could serve as a promising therapeutic target for addressing diabetes-related vascular disorders. In our study, we have demonstrated that DNMT1 exhibits overexpression in the wound margin tissues of patients with DFUs, as well as in the human dermal microvascular endothelial cells subjected to HG. Functional study showed that the overexpression of DNMT1 exacerbates the dysfunction of human dermal microvascular endothelial cells induced by HG. These data robustly support that HG acts as the upstream driver of DNMT1 overexpression, which subsequently mediates endothelial dysfunction. Of particular importance, our data demonstrated that overexpression of DNMT1 counteracts the restorative effects of GFOD1-AS1 knockdown on HG-induced dysfunction of human dermal microvascular endothelial cells. Therefore, we propose that DNMT1 is an effective molecule through which GFOD1-AS1 exerts its function.

Increasing evidence shows that lncRNA can act as a decoy, scaffold or guide for RBPs to affect their modification, stability, localization and activity, thereby participating in the occurrence and progression of a variety of diseases (Statello et al. 2021; Yao et al. 2022). Our research data demonstrated that GFOD1-AS1 interacted with DNMT1 to increase the stability of the DNMT1 protein. Ubiquitination, a pivotal post-translational modification, is essential for the regulation of protein homeostasis, with the ubiquitin-proteasome system responsible for approximately 80% of protein degradation (Wang and Maldonado 2006; Zhong et al. 2022). Our research data indicated that knockdown of GFOD1-AS1 leaded to the degradation of DNMT1 protein through the ubiquitin-proteasome system, suggesting that the DNMT1 protein stability is regulated by the ubiquitin-proteasome system, which is consistent with previous research findings (Fang et al. 2023; Zhang et al. 2023). Existing studies have demonstrated that lncRNA can regulate the degradation of DNMT1 protein by controlling the ubiquitination status of DNMT1 (Xu et al. 2019; Geng et al. 2021). For instance, lncRNA LUCAT1 interacts with DNMT1, inhibiting its degradation through the ubiquitin-proteasome pathway, thereby enhancing the DNMT1 protein stability and promoting the occurrence and progression of esophageal squamous cell carcinoma (Yoon et al. 2018). Consistent with the aforementioned research findings, our experimental results also demonstrated that GFOD1-AS1 directly interacted with DNMT1 to block the ubiquitination modification of DNMT1 protein, thereby regulating HG-induced human dermal microvascular endothelial cells dysfunction. However, the intrinsic and fine-tuned regulatory mechanisms by which the direct interaction between GFOD1-AS1 and DNMT1 blocks the ubiquitin degradation of DNMT1 have not been explored in this study.

Recent studies have shown that lncRNA can participate in the occurrence and development of a variety of diseases by competitively binding substrates with E3 ubiquitin ligases, blocking the ubiquitination and degradation of

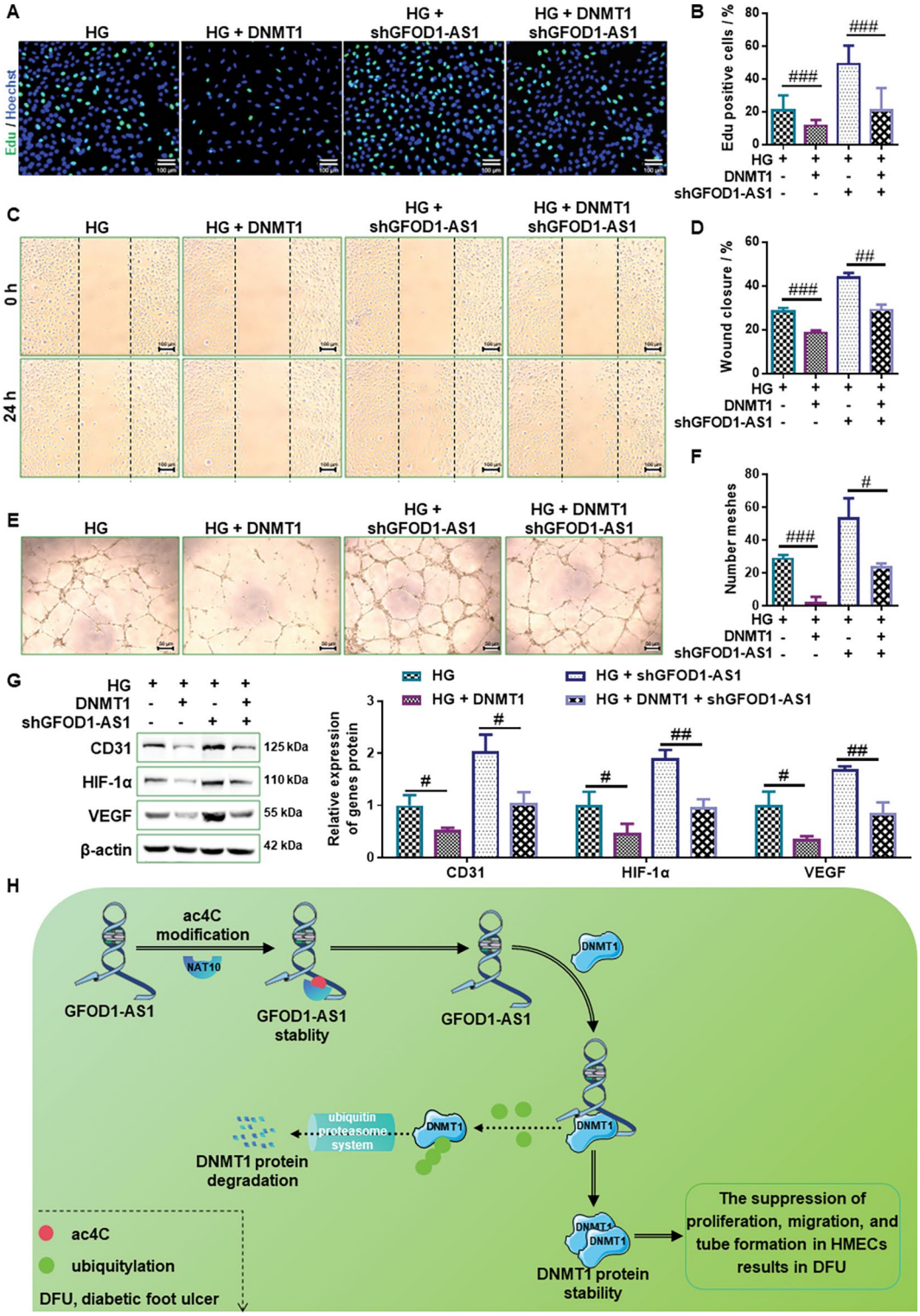

Fig. 5 GFOD1-AS1 knockdown mitigates high-glucose vascular endothelial cell injury by suppressing DNMT1 expression, and the detailed comparisons between high glucose and control groups provided in Figs. 1 and 2. (**A** and **B**) The EdU assay was used to measure the proliferation ability in the indicated HMEC-1 cells. Scale bar = 100 μm. (**C** and **D**) The wound healing assay was applied to detect the migration in the indicated HMEC-1 cells. Scale bar = 100 μm. (**E** and **F**) The tube formation assay was utilized to evaluate the angiogenic tube formation capacity in the indicated HMEC-1 cells. Scale bar = 50 μm. (**G**) Western blot analysis was conducted to assess the protein expression levels of angiogenic markers (VEGF, HIF-1α, and CD31) in the indicated HVEC cells. HG, high glucose; DNMT1, DNMT1 overexpression vector; shGFOD1-AS1, GFOD1-AS1 short hairpin RNA vector. (**H**) Schematic diagram of the mechanism by which GFOD1-AS1 promotes the dysfunction in microvascular endothelial cells of diabetic foot ulcers. $N = 3$, $^{\#}p < 0.05$, $^{\#\#}p < 0.01$, and $^{\#\#\#}p < 0.001$

substrates mediated by E3 ligase and enhancing the stability of substrate proteins. For example, lncRNA-ZXF1 directly binds to P21, blocking the binding site of E3 ubiquitin ligase CDC20 with its substrate P21, thus inhibiting the CDC20-mediated ubiquitination-degradation pathway of P21 and maintaining P21 protein stablilty, which in turn resists the occurrence and development of endometrial cancer (Kong et al. 2021). Additionally, recent research evidence indicates that lncRNA SNHG6 competitively binds to DNMT1 with ubiquitin-like with PHD and ring finger domains 1 (UHRF1), blocking the ubiquitination degradation of DNMT1 mediated by UHRF1, enhancing the stability of DNMT1 protein, thereby increasing the methylation level of the brain-derived neurotrophic factor (BDNF) promoter, and regulating depressive-like behaviors in hypothyroid mice (Yang et al. 2022). In the light of our findings and recent literature, we speculate that GFOD1-AS1 may compete with E3 ubiquitin ligase to bind DNMT1, block the ubiquitination and degradation of DNMT1 mediated by E3 ubiquitin ligase, thereby maintaining the stability of DNMT1 protein and leading to the occurrence and development of DFU. Building upon the findings of this study, future research will systematically explore this hypothesis through cellular, preclinical animal models, and clinical levels to uncover novel pathogenic mechanisms of DFU and develop innovative clinical treatment strategies. Furthermore, our data suggest that DNMT1 is a key mediator of high glucose-induced endothelial dysfunction, but the potential regulatory role of DNMT1 overexpression under normal glucose conditions remains unexplored. Future studies may investigate whether DNMT1 plays a glucose environment-dependent or independent role in microvascular homeostasis.

Conclusion

Our research findings suggest that GFOD1-AS1, modulated by NAT10-mediated ac4C modification, emerges as a promising therapeutic target for the treatment of challenging wounds associated with DFU. Mechanistically, GFOD1-AS1 directly interacts with DNMT1, blocking its ubiquitin degradation and maintaining DNMT1 protein stability, ultimately promoting the HG-mediated dysfunction of human dermal microvascular endothelial cells (Fig. 5H). These findings provide valuable clues for the development of new therapeutic strategies for DFU and point the way for future research.

Supplementary Information The online version contains supplementary material available at https://doi.org/10.1007/s10142-025-01617-x.

Author contributions Study design and planning: Jingjing Yuan, Wenjun YangData collection and curation: Lusha Li, Yang LvExperiments performance: Jingjing Yuan, Lusha Li, Yang LvManuscript writing: Jingjing Yuan, Wenjun YangAll author approved the final version of the manuscript.

Funding Not applicable.

Data availability No datasets were generated or analysed during the current study.

Declarations

Competing interests The authors declare no competing interests.

References

Arango D, Sturgill D, Alhusaini N, Dillman AA, Sweet TJ, Hanson G, Hosogane M, Sinclair WR, Nanan KK, Mandler MD, Fox SD, Zengeya TT, Andresson T, Meier JL, Coller J, Oberdoerffer S (2018) Acetylation of cytidine in mRNA promotes translation efficiency. Cell 175:1872–1886e24

Architha T, Juanitaa GR, Vijayalalitha R, Jayasuriya R, Athira G, Balamurugan R, Ganesan K, Ramkumar KM (2024) LncRNA NEAT1/miR-146a-5p Axis restores normal angiogenesis in diabetic foot ulcers by targeting MafG. Cells.;13

Armstrong DG, Tan TW, Boulton AJM, Bus SA (2023) Diabetic foot ulcers: A review. JAMA 330:62–75

Bian EB, Xiong ZG, Li J (2019) New advances of LncRNAs in liver fibrosis, with specific focus on lncRNA-miRNA interactions. J Cell Physiol 234:2194–2203

Chen L, Shen S, Wang S (2023) LncRNA SNHG16 knockdown promotes diabetic foot ulcer wound healing via sponging MiR-31-5p. Tohoku J Exp Med

Cui Z, Cong M, Yin S, Li Y, Ye Y, Liu X, Tang J (2024) Role of protein degradation systems in colorectal cancer. Cell Death Discov 10:141

Fang T, Jiao Z, You Y, Cao J, Wang C, Liu J, Zhao W (2023) Lenvatinib inhibited HCC cell migration and invasion through regulating the transcription and ubiquitination of UHRF1 and DNMT1. Biochem Pharmacol 210:115489

Fu W, Liang D, Wu X, Chen H, Hong X, Wang J, Zhu T, Zeng T, Lin W, Chen S (2022) Yan L and Ren M. Long noncoding RNA LINC01435 impedes diabetic wound healing by facilitating YY1-mediated HDAC8 expression. iScience 25:104006

Geng X, Zhao J, Huang J, Li S, Chu W, Wang WS, Chen ZJ, Du Y (2021) lnc-MAP3K13-7:1 inhibits ovarian GC proliferation in PCOS via DNMT1 Downregulation-Mediated CDKN1A

promoter hypomethylation. Mol Therapy: J Am Soc Gene Therapy 29:1279–1293
Gong S, Qiao H, Wang JY, Huang SY, He SW, Zhao Y, Tan XR, Ye ML, Li JY, Liang YL, Huang SW, Chen J, Zhu XH, Liu N, Li YQ (2024) Ac4C modification of LncRNA SIMALR promotes nasopharyngeal carcinoma progression through activating eEF1A2 to facilitate ITGB4/ITGA6 translation. Oncogene 43:2868–2884
Guo L, Xiao D, Xing H, Yang G, Yang X (2024) Engineered exosomes as a prospective therapy for diabetic foot ulcers. Burns Trauma 12:tkae023
Herman AB, Tsitsipatis D, Gorospe M (2022) Integrated LncRNA function upon genomic and epigenomic regulation. Mol Cell 82:2252–2266
Hernandez-Guedes A, Arteaga-Marrero N, Villa E, Callico GM, Ruiz-Alzola J (2023) Feature Ranking by Variational Dropout for Classification Using Thermograms from Diabetic Foot Ulcers. *Sensors (Basel, Switzerland)*.;23
Huang H, Huang Y (2024) USP7-stabilised HIPK2 promotes high glucose-induced endothelial cell dysfunctions to accelerate diabetic foot ulcers. Arch Physiol Biochem 130:984–991
Kang X, Kong F, Huang K, Li L, Li Z, Wang X, Zhang W, Wu X (2019) LncRNA MIR210HG promotes proliferation and invasion of non-small cell lung cancer by upregulating methylation of CACNA2D2 promoter via binding to DNMT1. Onco Targets Ther 12:3779–3790
Kong D, Hou Y, Li W, Ma X, Jiang J (2021) LncRNA-ZXF1 regulates P21 expression in endometrioid endometrial carcinoma by managing ubiquitination-mediated degradation and miR-378a-3p/PCDHA3 axis. Mol Oncol
Kopp F, Mendell JT (2018) Functional classification and experimental dissection of long noncoding RNAs. Cell 172:393–407
Li B, Luan S, Chen J, Zhou Y, Wang T, Li Z, Fu Y, Zhai A, Bi C (2020) The MSC-Derived Exosomal LncRNA H19 promotes wound healing in diabetic foot ulcers by upregulating PTEN via MicroRNA-152-3p. Mol Ther Nucleic Acids 19:814–826
Liu J, Zhang Y, Liu C, Jiang Y, Wang Z, Guo Z, Li X (2024) A single dose of VEGF-A circular RNA sustains in situ long-term expression of protein to accelerate diabetic wound healing. J Control Release 373:319–335
Lu Y, Liu X, Zhao J, Bie F, Liu Y, Xie J, Wang P, Zhu J, Xiong Y, Qin S, Yang F, Chen L, Xu Y (2023) Single-cell profiling reveals transcriptomic signatures of vascular endothelial cells in non-healing diabetic foot ulcers. Front Endocrinol (Lausanne) 14:1275612
Luo L, An Y, Geng K, Wan S, Zhang F, Tan X, Jiang Z, Xu Y (2023a) High glucose-induced endothelial STING activation inhibits diabetic wound healing through impairment of angiogenesis. Biochem Biophys Res Commun 668:82–89
Luo J, Cao J, Chen C, Xie H (2023b) Emerging role of RNA acetylation modification ac4C in diseases: current advances and future challenges. Biochem Pharmacol 213:115628
Peng WX, He PX, Liu LJ, Zhu T, Zhong YQ, Xiang L, Peng K, Yang JJ, Xiang GD (2021) LncRNA GAS5 activates the HIF1A/VEGF pathway by binding to TAF15 to promote wound healing in diabetic foot ulcers. Lab Invest 101:1071–1083
Rai V, Moellmer R, Agrawal DK (2022) Stem cells and angiogenesis: implications and limitations in enhancing chronic diabetic foot ulcer healing. Cells.;11
Rai V, Le H, Agrawal DK (2023) Novel mediators regulating angiogenesis in diabetic foot ulcer healing. Can J Physiol Pharmacol 101:488–501
Statello L, Guo CJ, Chen LL, Huarte M (2021) Gene regulation by long non-coding RNAs and its biological functions. Nat Rev Mol Cell Biol 22:96–118
Wang J, Maldonado MA (2006) The ubiquitin-proteasome system and its role in inflammatory and autoimmune diseases. Cell Mol Immunol 3:255–261
Wang Q, Liu J, You Z, Yin Y, Liu L, Kang Y, Li S, Ning S, Li H, Gong Y, Xu S, Pang D (2021) LncRNA TINCR favors tumorigenesis via STAT3-TINCR-EGFR-feedback loop by recruiting DNMT1 and acting as a competing endogenous RNA in human breast cancer. Cell Death Dis 12:83
Wang G, Zhang M, Zhang Y, Xie Y, Zou J, Zhong J, Zheng Z, Zhou X, Zheng Y, Chen B, Liu C (2022) NAT10-mediated mRNA N4-acetylcytidine modification promotes bladder cancer progression. Clin Translational Med 12:e738
Wang K, Wang Y, Shi W, Shen K, Tao K, Ling R, Huang Y, Fu X, Hu D (2024) Diagnosis and treatment of diabetic foot ulcer complicated with lower extremity vasculopathy: consensus recommendation from the Chinese medical association (CMA), Chinese medical Doctor association (CMDA). Diabetes Metab Res Rev 40:e3776
Wu Y, Cao Y, Liu H, Yao M, Ma N, Zhang B (2020) Remodelin, an inhibitor of NAT10, could suppress hypoxia-induced or constitutional expression of HIFs in cells. Mol Cell Biochem 472:19–31
Xu X, Lou Y, Tang J, Teng Y, Zhang Z, Yin Y, Zhuo H, Tan Z (2019) The long non-coding RNA Linc-GALH promotes hepatocellular carcinoma metastasis via epigenetically regulating Gankyrin. Cell Death Dis 10:86
Xu T, Hu L, Xie B, Huang G, Yu X, Mo F, Li W, Zhu M (2024) Analysis of clinical characteristics in patients with diabetic foot ulcers undergoing amputation and establishment of a nomogram prediction model. Sci Rep 14:27934
Xue W, Zhang Q, Chen Y, Zhu Y (2022) Hydrogen sulfide improves angiogenesis by regulating the transcription of pri-miR-126 in diabetic endothelial cells. Cells.;11
Yan C, Chen J, Yang X, Li W, Mao R, Chen Z (2021) Emerging roles of long Non-Coding RNAs in diabetic foot ulcers. Diabetes Metab Syndr Obes 14:2549–2560
Yan Q, Zhou J, Wang Z, Ding X, Ma X, Li W, Jia X, Gao SJ, Lu C (2023) NAT10-dependent N(4)-acetylcytidine modification mediates PAN RNA stability, KSHV reactivation, and IFI16-related inflammasome activation. Nat Commun 14:6327
Yang Z, Jiang S, Shang J, Jiang Y, Dai Y, Xu B, Yu Y, Liang Z, Yang Y (2019) LncRNA: Shedding light on mechanisms and opportunities in fibrosis and aging. *Ageing Res Rev*.;52:17–31
Yang H, Jia W, Zhang DP, Xu YX, Wang F, Wang N, Zhu DF (2022) Long non-coding RNAs and small nucleolar RNA host gene 6 contribute to the depression-like behavior of hypothyroid mice by promoting methylation of the brain-derived neuropathic factor promoter that is mediated by DNA methyltransferase 1. J Physiol Pharmacology: Official J Pol Physiological Soc.;73
Yao ZT, Yang YM, Sun MM, He Y, Liao L, Chen KS, Li B (2022) New insights into the interplay between long non-coding RNAs and RNA-binding proteins in cancer. Cancer Commun (London England) 42:117–140
Yi Q, Feng J, Lan W, Shi H, Sun W, Sun W (2024) CircRNA and lncRNA-encoded peptide in diseases, an update review. Mol Cancer 23:214
Yoon JH, You BH, Park CH, Kim YJ, Nam JW, Lee SK (2018) The long noncoding RNA LUCAT1 promotes tumorigenesis by controlling ubiquitination and stability of DNA methyltransferase 1 in esophageal squamous cell carcinoma. Cancer Lett 417:47–57
Yu XM, Li SJ, Yao ZT, Xu JJ, Zheng CC, Liu ZC, Ding PB, Jiang ZL, Wei X, Zhao LP, Shi XY, Li ZG, Xu WW, Li B (2023) N4-acetylcytidine modification of LncRNA CTC-490G23.2 promotes cancer metastasis through interacting with PTBP1 to increase CD44 alternative splicing. Oncogene 42:1101–1116
Yu C, Chen Y, Luo H, Lin W, Lin X, Jiang Q, Liu H, Liu W, Yang J, Huang Y (2024) NAT10 promotes vascular remodelling via mRNA ac4C acetylation. Eur Heart J.:ehae707
Zhang Y (2024) LncRNA-encoded peptides in cancer. J Hematol Oncol 17:66

Zhang N, Gao X, Yuan Q, Fu X, Wang P, Cai F, Liu H, Zhang J, Liang H, Nie Y, Deng J (2023) E3 ubiquitin ligase RNF180 prevents excessive PCDH10 methylation to suppress the proliferation and metastasis of gastric cancer cells by promoting ubiquitination of DNMT1. Clin Epigenetics 15:77

Zhang Y, Liu H, Yang Y, Feng C, Cui L (2024) Incidence and risk factors for amputation in Chinese patients with diabetic foot ulcers: a systematic review and meta-analysis. Front Endocrinol (Lausanne) 15:1405301

Zhao J, Yang S, Shu B, Chen L, Yang R, Xu Y, Xie J, Liu X, Qi S (2021) Transient high glucose causes persistent vascular dysfunction and delayed wound healing by the DNMT1-Mediated Ang-1/NF-κB pathway. J Invest Dermatol 141:1573–1584

Zhong T, Lei K, Lin X, Xie Z, Luo S, Zhou Z, Zhao B, Li X (2022) Protein ubiquitination in T cell development. Front Immunol 13:941962